

Prospects for the detection of gamma rays using Cherenkov telescopes enhanced by a ground array observatory

C. Alispach^a, A. Araudo^b, A. Bakalová^b, M. Balbo^a, V. Beshley^c, J. Blažek^b, J. Borkowski^d, T. Bulík^f, F. Cadoux^a, S. Casanova^e, A. Christov^b, J. Chudoba^b, L. Chytká^g, P. Čechvala^{b,*}, P. Dědic^b, Y. Favre^a, M. Garczarczyk^h, L. Gibaudⁱ, T. Gieras^e, E. Głowackiⁱ, P. Hamal^g, M. Heller^a, M. Hrabovský^g, P. Janeček^b, M. Jelínek^j, V. Jílek^g, J. Juryšek^b, V. Karas^k, B. Lacave^a, E. Lyard^l, D. Mandát^b, W. Marek^e, S. Michałowski^e, M. Miroňⁱ, R. Moderski^d, T. Montaruli^a, A. Muraczewski^d, S. R. Muthyalu^b, A. L. Müller^b, A. Nagai^a, K. Nalewajski^e, D. Neise^m, J. Niemiec^e, M. Nikołajukⁱ, V. Novotný^{b,n,*}, M. Ostrowski^o, M. Palatka^b, M. Pech^b, M. Prouza^b, P. Schovánek^b, T. Schulz^b, V. Sliusar^l, J. Srbaⁱ, Ł. Stawarz^o, R. Sternberger^h, M. Stodulska^a, J. Świerblewski^e, P. Świerk^e, J. Štrobly^l, T. Tavernier^b, P. Trávníček^b, I. Troyano Pujadas^a, J. Vícha^b, R. Walter^l, K. Ziętara^o, **(SST-1M Collaboration)**, R. Conceição^p, L. Gibilisco^p, M. Pimenta^p and B. Tomé^p

^aDépartement de Physique Nucléaire, Faculté de Sciences, Université de Genève, 24 Quai Ernest Ansermet, Genève, 1205, Switzerland

^bFZU - Institute of Physics of the Czech Academy of Sciences, Na Slovance 1999/2, Prague, 18200, Czech Republic

^cPidstryhach Institute for Applied Problems of Mechanics and Mathematics, National Academy of Sciences of Ukraine, 3-b Naukova St., Lviv, 79060, Ukraine

^dNicolaus Copernicus Astronomical Center, Polish Academy of Sciences, ul. Bartycka 18, Warsaw, 00-716, Poland

^eInstitute of Nuclear Physics, Polish Academy of Sciences, Krakow, 31-342, Poland

^fAstronomical Observatory, University of Warsaw, Al. Ujazdowskie 4, Warsaw, 00-478, Poland

^gPalacký University Olomouc, Faculty of Science, 17. listopadu 50, Olomouc, 77900, Czech Republic

^hDeutsches Elektronen-Synchrotron (DESY), Platanenallee 6, Zeuthen, 15738, Germany

ⁱFaculty of Physics, University of Białystok, ul. K. Ciołkowskiego 1L, Białystok, 15-245, Poland

^jAstronomical Institute of the Czech Academy of Sciences, Fričova 298, Ondřejov, 25165, Czech Republic

^kAstronomical Institute of the Czech Academy of Sciences, Boční II 1401, Prague, 14100, Czech Republic

^lDépartement d'Astronomie, Faculté de Science, Université de Genève, Chemin d'Ecogia 16, Versoix, 1290, Switzerland

^mETH Zurich, Institute for Particle Physics and Astrophysics, Otto-Stern-Weg 5, Zurich, 8093, Switzerland

ⁿInstitute of Particle and Nuclear Physics, Faculty of Mathematics and Physics, Charles University, V Holešovičkách 2, Prague, 18000, Czech Republic

^oAstronomical Observatory, Jagiellonian University, ul. Orla 171, Krakow, 30-244, Poland

^pPhysics Department, Instituto Superior Técnico, Universidade de Lisboa and LIP - Laboratório de Instrumentação e Física Experimental de Partículas, Av. Prof. Gama Pinto 2, Lisboa, 1649-003, Portugal

ARTICLE INFO

Keywords:

gamma rays

flux sensitivity

IACT

WCD

SST-1M

SWGO

ABSTRACT

We consider the Single-Mirror Small-Size imaging atmospheric Cherenkov Telescopes (SST-1M) to be located inside a high-altitude array of Water-Cherenkov Detectors (WCDs) inspired by the Southern Wide-field Gamma-ray Observatory (SWGO). For such a hybrid observatory, using detailed Monte Carlo simulations, we show an improvement in the flux sensitivity of monocular and stereoscopic SST-1M observation by about 60% and 30% above 10 TeV, respectively, due to the improved gamma/hadron separation when additional parameters from the WCD array are used. We also discuss further benefits of the hybrid SWGO concept and its technical challenges.

1. Introduction

Observations of very-high-energy (VHE) gamma rays provide crucial insights into the most energetic astrophysical accelerators. Ground-based detection of VHE gamma rays utilize either an array of particle detectors or Imaging air-Cherenkov telescopes (IACTs). However, each technique comes with its limitations. While particle-detector arrays

provide a wide field of view and a high duty cycle with limited angular resolution, the IACTs have excellent sensitivity and resolution with a limited field of view and duty cycle. A hybrid detection approach combines a particle-detector array with IACTs, offers a way to overcome these limitations, and thus can improve the capabilities of wide-field gamma-ray observatories. The potential of such a hybrid detection configuration has already been explored by the LHAASO Collaboration in view of the LACT IACT array [1].

*Corresponding author

✉ czechvala@fzu.cz (P. Čechvala); vladimir.novotny@matfyz.cuni.cz (V. Novotný)

ORCID(s): 0009-0009-2107-1848 (P. Čechvala); 0000-0002-4319-4541 (V. Novotný)

In this paper, we present a simulation study of a hybrid-detection concept combining two IACTs—modeled as Single-Mirror Small-Size imaging atmospheric Cherenkov Telescopes (SST-1Ms) [2, 3] utilizing a silicon-photomultiplier camera [4]—with a particle-detector array based on the design concept of the Southern Wide-field Gamma-ray Observatory (SWGO) [5, 6]. Preliminary results of this study were presented in Ref. [7].

The paper is structured as follows: Section 2 describes the simulation setup; Section 3 presents the observables used to enhance gamma/hadron (γ/h) separation capability; and the main results concerning the sensitivity of a hybrid SWGO-like array equipped with SST-1M in monocular and stereoscopic modes are presented in Section 4. The general discussion of scientific benefits of such a hybrid array is given in Section 5; and the technical aspects of a high-elevation operation of SST-1M is briefly discussed in Section 6. Section 7 summarizes the obtained findings and describes the future outlook of this work.

2. Simulation setup

To estimate the performance of a realistic hybrid detector consisting of air-Cherenkov telescopes and the ground array made of water-Cherenkov detectors (WCDs), we prepared a three-step set of detailed Monte Carlo (MC) simulations. The development of air showers and the consequent production of Cherenkov light was calculated in CORSIKA v7.7402 [8]. We employed UrQMD [9] as the low-energy (<80 GeV) interaction model and QGSJet II-04 [10] was used for interactions at higher energies. Subsequently, the response of the SST-1M telescopes was simulated in sim_telarray v2021-12-25 [11], also taking into account the light attenuation in the atmosphere. In the third step, the WCD signals were evaluated using the simplified framework adopted from Ref. [12]. Within the framework, cylindrical WCDs are placed on a regular grid and the signal from through-going particles is calculated from a parametrized model of the detectors, taking into account fluctuations of the signal.

The particle-detector array consisted of 9997 WCDs, each covering 12.6 m^2 and equipped with 3 photomultiplier tubes, spread over a total area of approximately 1 km^2 in a uniform triangular grid, implying a fill factor (FF) of 12.5%. This very large number of WCDs and large FF were deliberately chosen to minimize border effects and potential reconstruction artifacts, while an optimized array size and possibly a gradient in FF will be used in reality to balance cost and performance across the full energy range. However, such considerations are beyond the scope of the present paper. Motivated by the future SWGO site [6], we set the simulated altitude to 4700 m and adjusted the atmospheric density profile, together with the geomagnetic field, to the Pampa la Bola site located in the Atacama Astronomical Park, Chile.

Two identical SST-1M telescopes were placed symmetrically around the center of the particle-detector array, 110 m apart in the North-South direction. Following the

detailed study of the SST-1M response in Ref. [3], night-sky background simulations with a photon rate of 72 MHz were performed. This value corresponds to the response of real silicon photomultipliers under low night-sky brightness expected at the high-altitude site. The atmosphere transmissivity set in sim_telarray was calculated using MODTRAN [13] for Pampa la Bola. Showers with a zenith angle of 20° , coming from the North, were simulated to benchmark low zenith angle observations.

The IACT simulations were processed using an open source software sst1mpipe v0.7.4¹ [14] developed for the calibration and air-shower reconstruction of SST-1M. Minor modifications to the used version of sst1mpipe were made in order to account for the selected site. Random Forests [15], used for event reconstruction, were trained on MC-simulated diffuse protons and gamma rays, while the response to a point-like source was calculated using point-like gammas. The primary particles, generated according to the energy spectral shape $\frac{dN}{dE} \propto E^{-2}$, have an energy between 200 GeV and 631 TeV, and 400 GeV and 1100 TeV for gamma rays and protons, respectively, to account for the migration of background events into the analyzed energy range. To cover the whole 9° field of view of SST-1M in the case of diffuse samples, showers are simulated up to 5° from the pointing axis of the telescopes. Events are evenly distributed in the area up to the impact distance of 1032 m from the array center, while the radius of the 1 km^2 particle-detector array was 565 m. Assuming that only showers with a core inside the WCD array can be reasonably analyzed, events with a core distance greater than 565 m are not used in the WCD array-enhanced analysis. In this case, only about $\approx 2\%$ of the reconstructed gamma rays are discarded, demonstrating that the array size is sufficient to adequately cover the effective area of the SST-1M telescopes in the configuration considered.

3. Particle-detector array observables

In this work, we use the information from the particle-detector array to enhance the γ/h separation capability of the SST-1M telescopes. This enhancement stems mainly from the sensitivity of the WCD array to the muon content of air showers, which is almost absent for gamma-ray primaries but substantial for those of hadronic origin. To study potential improvement, we first focus on adding the γ/h separation variables obtained from the WCD array to the standard SST-1M analysis. Exploitation of the complete ground-array information could yield better performance but would be subject to further work and is discussed in Section 5. Instead, we extracted only two γ/h separation variables, LCm and P_{tail}^α , using a simplified framework from Ref. [12], under the assumption that the shower footprints are contained within the array.

The first variable, LCm [12], quantifies the azimuthal fluctuations of the ground signal. On the one hand, gamma-ray induced showers are dominated by the electromagnetic

¹<https://github.com/SST-1M-collaboration/sst1mpipe>

component and therefore produce a rather smooth lateral signal distribution. On the other hand, hadronic showers exhibit stronger azimuthal fluctuations of the signal due to their more complex structure. For a detailed definition of the LCm variable and its performance, see Refs. [12, 16, 17].

The second variable extracted from the WCD array is P_{tail}^α [18], which represents the extent to which the detectors record a signal significantly above the average of all detectors at a comparable core distance. This parameter has been shown to be well correlated with the total number of muons and thus provides an efficient γ/h separation variable that allows us to obtain a high-purity gamma samples.

Both variables are reconstructed for shower energies greater than 10 TeV as suggested in Ref. [12]. However, in principle, other methods and variables that correlate with the number of muons can also be introduced at lower energies as shown in Refs. [6, 19]. Thus, in addition to the two variables reconstructed from the particle-detector array, we also use for illustration purposes the true number of muons in the showers, N_μ , obtained directly from CORSIKA simulations at the ground level within a 1 km^2 circle around the shower core. Although this variable is not usable in real data, it provides insight into which of the proxies more closely approaches its performance.

4. SST-1M with enhanced gamma/hadron separation

In this section, we quantify the expected performance improvement of SST-1M telescopes when supplemented with a SWGO-like array. We focus on the impact of the additional WCD-array information on γ/h separation and on the resulting sensitivity of the combined system, presenting the results separately for monocular and stereoscopic SST-1M operation modes.

The evaluation is performed by comparing the baseline SST-1M reconstruction with the hybrid setup described in Sections 2 and 3. The WCD-array discrimination variables, P_{tail}^α and LCm , were incorporated as additional features in the Random Forest (RF) classifier trained within `sst1mpipe` to perform γ/h separation, represented by the *gammaness* parameter [3]. The trained RF model was subsequently applied to an independent test MC sample. Because the parameterizations used to calculate LCm and P_{tail}^α are energy dependent, we need to provide a reference energy to the framework. Rather than using the MC value, the energy estimate reconstructed by the pipeline using a separate RF regressor was used to compute P_{tail}^α and LCm , thereby propagating the realistic energy-resolution effects of the reconstruction chain into these parameters.

To assess the separation capability of the hybrid approach, we employ Receiver Operating Characteristic (ROC) curves and their integral metrics, and we report the corresponding signal efficiency and background rejection factors for representative working points to enable a direct comparison with the baseline configuration. To evaluate

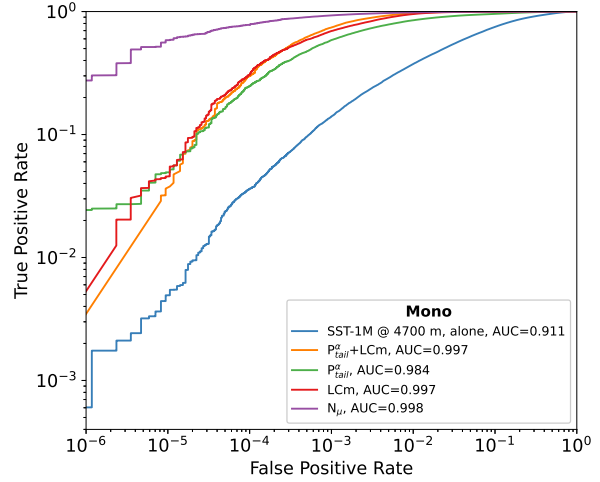


Figure 1: ROC curves in the monocular observation regime. Shown for a single SST-1M telescope alone (blue) and for SST-1M together with γ/h discrimination parameters obtained from the particle-detector array, including P_{tail}^α (green), LCm (red), both P_{tail}^α and LCm (orange), and true number of muons N_μ (purple). All curves are shown for energies above 10 TeV.

the final performance of the SST-1M telescopes, we apply standard event-quality selections following Ref. [3]: a Hillas' intensity cut of >45 photoelectrons and a leakage cut of <0.7 . An energy-dependent gammaness cut is then applied to retain a fixed efficiency for gamma-ray selection of 60% in both the monocular and stereoscopic analyses, while imposing an upper limit of 0.95 on the cut value. Finally, to maximize the detection significance, an energy-dependent θ^2 cut (the squared angular distance between the reconstructed shower direction and the source position) is optimized independently for the two observation regimes, yielding subsequent efficiencies for gamma-ray selection of 50% and 68% for the monocular and stereoscopic analysis, respectively.

Finally, we translate the changes in γ/h separation performance into sensitivity estimates for the hybrid array and discuss the conditions under which the hybrid concept yields the largest gains with respect to the baseline SST-1M reconstruction. Because the SST-1M performance depends strongly on the telescope trigger multiplicity, we present the results for monocular and stereoscopic configurations separately.

4.1. Monocular performance

In this Section, we estimate the performance of a single SST-1M telescope in the middle of the SWGO-like array. Since the P_{tail}^α and LCm discriminators are, by design, intended to operate at high energies—typically above 10 TeV—the ROC curves shown in Fig. 1 are evaluated only for events with energies above this threshold, ensuring a fair and meaningful comparison.

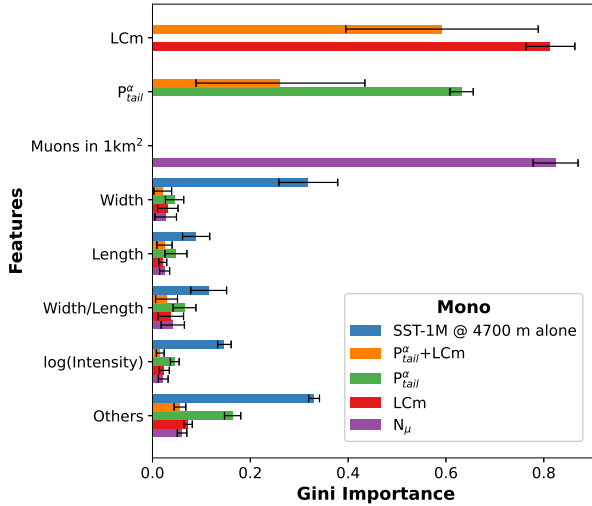


Figure 2: Gini importance of features used in the Random Forests classifiers that separate γ rays from hadrons. The analyses that use sole SST-1M telescope (blue) and SST-1M telescope with additional information from the particle-detector array are shown: true N_μ (purple), LCm (red), P_{tail}^α (green), and $P_{tail}^\alpha + LCm$ (orange). Only the most important features are depicted, while the contribution of the rest of them, listed in the text, is summed and shown as Others.

To illustrate how much information in the gammaness comes from individual variables, we show the Gini importance [15] of individual reconstruction parameters for different γ/h classifiers in Fig. 2. Only the most important features are visualized, while the complete list of analyzed parameters follows. In the case of the standard SST-1M reconstruction, features derived from the Hillas' parameterization are used, namely the log of the intensity, width, length, width/length ratio, skewness, kurtosis, timing slope, leakage, and coordinates of the shower center of gravity in the FoV (x,y). A highly performing variable driving the classification for gamma-hadron discrimination is Hillas' width, which measures the spread of a shower on the camera; see Ref. [3] for more details.

The decision relies heavily on the number of muons, N_μ , when included, consistent with the fact that gamma-ray showers are expected to produce fewer muons than hadronic showers. Similarly, P_{tail}^α and LCm also dominate the decision logic overall when used due to their correlation with N_μ . When both LCm and P_{tail}^α are present in the analysis, LCm is more important than P_{tail}^α , demonstrating its better γ/h separation capability in this particular dense layout.

Using the RF models built above, we evaluated the sensitivity of a single SST-1M to a point-like source at 20° zenith angle, observed for 50 h, utilizing different γ/h separation methods. The sensitivity is defined according to the standard rules in gamma astronomy, presented in Ref. [20], as a flux for which the detection with 5σ statistical significance should be achieved, at least ten excess events surviving cuts are demanded, and the signal to background ratio must be of

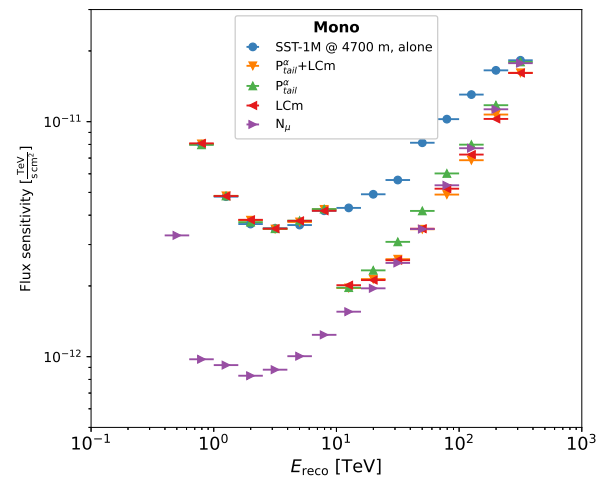


Figure 3: Flux sensitivity for a sole SST-1M telescope (blue) and one SST-1M with the additional information from the particle-detector array. The color coding is the same as in Fig 1. A point-like source at the zenith angle of 20° observed for 50 h is assumed.

at least 5%, everything evaluated separately in each energy bin. As clearly visible in Fig. 3, the sensitivity is significantly better for additional γ/h separation variables. The N_μ estimates illustrate the potential of future γ/h separation methods at low energies, while the performance of LCm and P_{tail}^α shows their impact at energies greater than ≈ 10 TeV. Interestingly, the LCm variable even surpasses N_μ at ultra-high energies as discussed in Ref. [17].

4.2. Stereoscopic performance

In the case of two SST-1M telescopes, additional parameters derived from the stereoscopic analysis, i.e., the distance of the impact point from the telescopes and the distance from the center of the IACT array to the shower maximum, h_{\max} , were included in the RF reconstruction described in Ref. [3]. Although the differences in the Gini importance of individual features of the γ/h classifiers are small, we show them in Fig. 5 for completeness. The ROC curves and flux sensitivities for the stereoscopic case are shown in Figs. 4 and 6, respectively. The improvement in sensitivity resulting from enhanced γ/h discrimination is less pronounced than that observed in the monocular case, primarily due to the inherently more precise reconstruction of the standalone SST-1M stereoscopic configuration, which leaves less room for improvement. Nevertheless, similar to the monocular performance, LCm surpasses N_μ at energies around 100 TeV where it was specifically tuned in Ref. [17].

To illustrate the scaling of sensitivity with observation time, we evaluated the combined $LCm + P_{tail}^\alpha$ sensitivity for 5, 50, and 500 h in Fig. 7. In the ultra-high-energy regime (> 100 TeV), the measurement is effectively background-free, thus being limited by the requirement of 10 detected photons in each energy bin as introduced in Ref. [20].

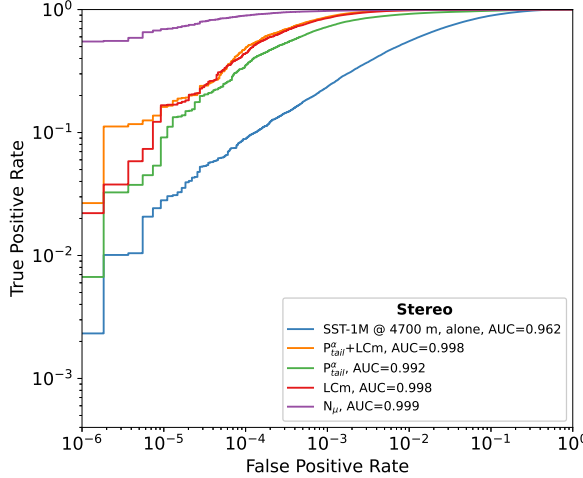


Figure 4: ROC curves in the stereoscopic observation regime. Shown for a pair of SST-1M telescopes alone (blue) and for SST-1Ms together with γ /h discrimination parameters similarly to Fig. 1. All curves are shown for energies above 10 TeV.

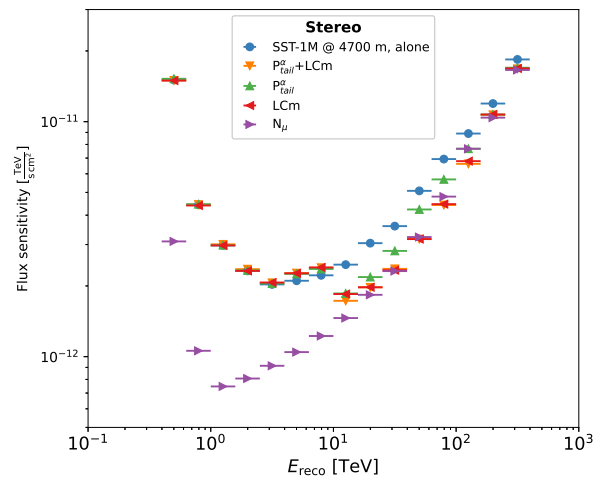


Figure 6: Flux sensitivity for two SST-1M telescopes (blue) and SST-1M telescopes with the additional information from the particle-detector array. The color coding and the observation parameters are the same as in Fig 3.

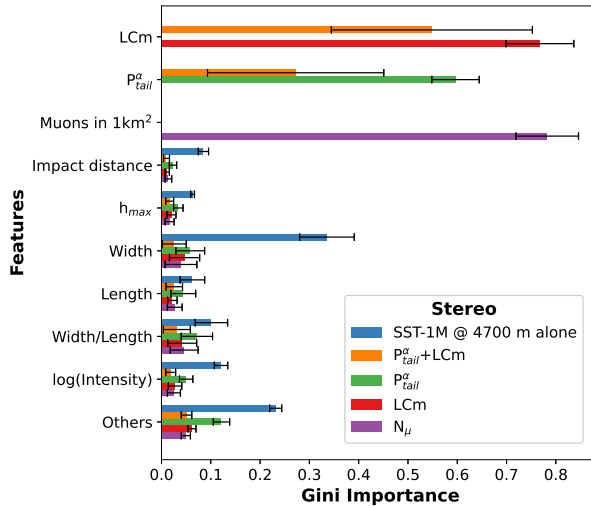


Figure 5: Gini importance of features used in the Random Forests classifiers when stereoscopic observation is assumed. Identical color coding as in Fig. 2 is used, as well as the summed quantities in Others are the same.

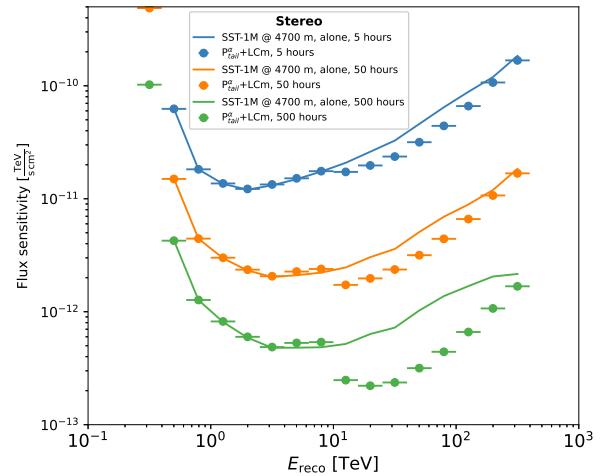


Figure 7: Evolution of the flux sensitivity with increasing observation time for the stereoscopic analysis enhanced with $LCM+P^a_tail$ γ /h separation. The same point-like source as in Figs. 3 and 6 was used. The lines represent sensitivities without WCD-array information.

5. Other benefits of hybrid detection

Besides the improvement of γ /h separation of SST-1M when the information from SWGO-like array is at disposal, as illustrated in the previous section, we briefly discuss the following scientific benefits of a hybrid combination of SWGO with SST-1M telescope(s).

- **Primary Identification:** a multi-parameter combination of primary-sensitive variables obtained from both techniques could improve the γ /h separation at all energies, not only above 10 TeV as investigated in

Section 4. Moreover, classification of charged cosmic-ray primaries can be studied. Important aspects could also be the cross-checks of the Machine-Learning predictions that are envisaged to be used for the air-shower reconstruction or γ /h separation at the SWGO by independent IACT methods.

- **Energy Calibration:** around energies of about 10 TeV, SST-1M telescopes operated at the SWGO site could provide an effective cross-calibration tool, offering better energy resolution (about 20% in monocular

mode and 15% in stereo regime, see Ref. [21]) and lower systematic uncertainty (about 10% or below as estimated in Ref. [2]). This could help to refine the absolute energy scale of the primary SWGO detector. In comparison, the main SWGO array is expected to achieve an energy resolution of about 15% or worse, see Ref. [6], and an energy-scale uncertainty of about 10% or worse, which is strongly dependent on energy and observation time when inferred from the Moon-shadow method [22].

- **Follow-up Observation:** the hybrid setup enables immediate follow-up observations by SST-1M on transient or variable sources detected by the wide-field SWGO, providing crucial spectral and morphological data due to its finer angular resolution (less than 0.15° and 0.10° in monocular and stereo regime, respectively, see Ref. [21]), complementing the SWGO main array's survey capabilities with angular resolution of 0.12° or worse as estimated in Ref. [6]. Although follow-up observations can be made from other sites as well, the integration of IACTs into SWGO can decrease the reaction time to seconds.
- **Geometry Reconstruction:** in a combined analysis, the SST-1M data can constrain the air-shower geometry for energies $\sim 1\text{--}10\text{ TeV}$, where the SST-1M reconstruction is performing very well, see Ref. [21], potentially leading to an improvement in the overall angular resolution for coincident events. The core resolution of the main SWGO array reaching values below 10 meters above 3 TeV, see Ref. [6], together with the angular resolution of the SST-1M telescopes could provide significant improvement in the air-shower geometry reconstruction for the combined analysis. Another important aspect would also be an independent cross-check of the angular resolution of the SWGO array using the SST-1M telescopes.

In general, the scientific advantages of adding imaging atmospheric Cherenkov telescopes (IACTs) to a wide-field water-Cherenkov-detector (WCD) array must be weighted against the logistical, operational, and financial implications of deploying and maintaining such specialized instrumentation. The installation, calibration, maintenance, and continuous operation of IACTs typically require dedicated technical expertise and infrastructure, increasing the overall operational complexity of the observatory. Implementing an IACT subsystem can therefore demand substantial project resources, including capital investment, specialized on-site personnel, and tailored facilities.

A further consideration is the duty cycle: while WCD arrays can operate with near-continuous uptime, IACT observations are traditionally restricted to clear nights and low-moon conditions, resulting in a significantly lower effective duty cycle. Consequently, performance gains enabled by IACT information are available only during a fraction of the total observation time. Nevertheless, modern IACT cameras

employing silicon photomultipliers, see Ref. [4], can tolerate high night-sky background levels and may extend operations into bright-moon conditions, partially mitigating this limitation.

Ultimately, the case for incorporating IACTs into a WCD-based observatory depends on whether the additional scientific return—such as improved γ/h separation, enhanced energy calibration and cross-validation, and more sensitive follow-up observations—provides sufficient benefit to justify the associated costs and operational overhead.

6. Technical aspects of operating SST-1M telescopes at the SWGO site

To ensure safety, full sky coverage, and reliable performance, specific spatial and infrastructural requirements need to be met, and also local environmental conditions must be considered, as they impose critical constraints that the integration of the system at the chosen site of Pampa La Bola, see Section 2, must accommodate. A fenced area of approximately $20 \times 30\text{ m}^2$ is required around the telescope structure to restrict unauthorized access during the operation. The size of the area is defined by the designated orientation of the parking position, typically pointing south, and a safe zone during the operation. Furthermore, to access all potential sources within the operational limits from 0° to 50° in zenith and 0° to 360° in azimuth in a clear, free field-of-view, the entire volume must be free from obscuration by any nearby infrastructure. In the proximity of the telescope area an enclosure is required for the telescope's local control and data acquisition electronics. A reinforced concrete platform, anchored to the underlying terrain, serves as the foundation of the telescope and needs to provide dynamic stability during the operations as well as structural integrity against high wind loads or possible seismic activity. Auxiliary foundation structures include a docking station foundation for the camera system, a small concrete pedestal for housing associated electronics and a loading platform. The telescope site itself as well as its access route and immediate surroundings must be sufficiently clear to allow the installation of the SST-1M using a 15-ton mobile crane and a 4-ton forklift.

According to the measurements performed at the Pampa La Bola site in 4700 m altitude and analyzed during the SWGO site selection process, the telescope must be able to withstand long periods with temperatures between -5°C and 0°C with short-term extremes dropping below -20°C during winter. The reduced air pressure at high altitude diminishes convective heat transfer efficiency, therefore influencing the cooling performance required for the camera system during operation. However, a closed-loop chiller system connected to a large underground water reservoir, acting as a passive heat sink, can efficiently dissipate the excess heat via a liquid medium. Furthermore, drive motors must operate reliably at low temperatures. The current SST-1M setup is not designed for so low air pressure and temperature, but the development of the necessary adaptation is

ongoing, including the refurbishment of the cooling system and potential use of heaters for the motors.

For safety reasons, the SST-1M operates at wind speeds below 50 km/h. At higher wind speeds, the telescope must be stowed in its parking position, where it can withstand gusts of up to 150 km/h. The use of back-coated mirror technologies introduced in Ref. [23] will mitigate substantially the progressive loss of the mirror reflectivity that is caused by the impact of small dust particles carried by high-velocity winds, despite it will reduce slightly the overall optical efficiency.

A stable 3-phase 400 V AC power supply is required to run the telescope's motors, cooling units, and electronic subsystems. High-speed data transfer for event acquisition slow-control communication has to be provided through an optical fiber connection. The core IT infrastructure comprises network switches, camera servers, and processing servers for on-site data analysis and preliminary data archiving. These systems will be consolidated within a single 42 U server rack housed in a temperature-controlled enclosure adjacent to the primary SWGO IT facilities. The total power consumption is defined by the IT system and the telescope system itself. The IT system requires a constant power consumption of 1 kW, which is independent of the number of telescopes. For a single SST-1M telescope, the power demand is estimated at 2 kW in standby mode and approximately 4 kW during operation, with a peak instantaneous power level of up to 8.5 kW. Assuming a daily duty cycle of 14 hours in standby and 10 hours in operation, the resulting average daily energy consumption is approximately 70 kWh.

Another critical operational aspect is the required data transfer rate and storage capacity. A single SST-1M telescope stores approximately 500 GB per observation night, whereas the daily data volume recorded by a WCD array is about 2.5 TB according to Ref. [24]. Given that IACTs cannot operate every night, they account for an additional data-handling capacity of approximately 10% per telescope.

7. Summary

In this work, we have demonstrated through detailed simulations an improvement in the performance of SST-1M telescopes—in both stereoscopic or monocular modes—when operated in a hybrid mode with a gamma-ray observatory made of water-Cherenkov detectors, located at a high-altitude of 4700 m a.s.l. The monocular and stereoscopic flux sensitivities of SST-1M have been improved by about 60% and 30% above 10 TeV, respectively, due to the enhanced γ/h separation capability when the LCm parameter of the WCD array was used. There are also other benefits of such a hybrid SWGO concept when multiple IACTs and WCDs are combined in a single observatory, including energy calibration of WCD array by SST-1M, fast follow-up studies of transients by SST-1M or mutual cross-checks of reconstructed air-shower observables. The main technical aspects that need to be considered for such a high-altitude observatory equipped with the SST-1M telescope(s) are the new design for cooling

of the camera, the drive operation, wind-speed alerts to park the telescope in time, and an extra energy consumption of about 70 kWh a day.

Acknowledgments

This publication was created as part of the projects funded in Poland by the Minister of Science based on agreements number 2024/WK/03 and DIR/WK/2017/12. The construction, calibration, software control and support for operation of the SST-1M cameras is supported by SNF (grants CRSII2_141877, 20FL21_154221, CRSII2_160830, _166913, 200021-231799), by the Boninchi Foundation and by the Université de Genève, Faculté de Sciences, Département de Physique Nucléaire et Corpusculaire. The Czech partner institutions acknowledge support of the infrastructure and research projects by Ministry of Education, Youth and Sports of the Czech Republic (MEYS) and the European Union funds (EU), MEYS LM2023047, EU/MEYS CZ.02.01.01/00/22_008/0004632, CZ.02.01.01/00/22_010/0008598, Co-funded by the European Union (Physics for Future – Grant Agreement No. 101081515), and Czech Science Foundation, GACR 23-05827S. The Portuguese contribution was supported by FCT - Fundação para a Ciência e a Tecnologia, I.P. OE., by PRT/BD/154192/2022 [DOI] and 2023.18160.ICDT [DOI].

References

- [1] Z. Zhang, R. Yang, S. Zhang, L. Yin, J. Liu, Y. Wang, L. Ma, Z. Cao, Prospects for joint reconstruction of imaging air Cherenkov telescope array and extensive air shower array, *JHEP* 43 (2024) 280–285. doi:10.1016/j.jheap.2024.07.012.
- [2] C. Alispach, et al., The SST-1M imaging atmospheric Cherenkov telescope for gamma-ray astrophysics, *JCAP* 02 (2) (2025) 047. doi:10.1088/1475-7516/2025/02/047.
- [3] C. Alispach, et al., Observation of the Crab Nebula with the Single-Mirror Small-Size Telescope stereoscopic system at low altitude, *Astron. Astrophys.* 699 (2025) A255. doi:10.1051/0004-6361/202555292.
- [4] M. Heller, et al., An innovative silicon photomultiplier digitizing camera for gamma-ray astronomy, *Eur. Phys. J. C* 77 (1) (2017) 47. doi:10.1140/epjc/s10052-017-4609-z.
- [5] P. Huentemeyer, S. BenZvi, B. Dingus, H. Fleischhacker, H. Schoorlemmer, T. Weisgarber, The Southern Wide-Field Gamma-Ray Observatory (SWGO): A Next-Generation Ground-Based Survey Instrument, in: *Bulletin of the American Astronomical Society*, Vol. 51, 2019, p. 109. doi:10.48550/arXiv.1907.07737.
- [6] P. Abreu, et al., Science Prospects for the Southern Wide-field Gamma-ray Observatory: SWGO, *arXiv e-prints* (Jun. 2025). doi:10.48550/arXiv.2506.01786.
- [7] A. Bakalová, et al., Hybrid concept of detection for a wide-field gamma-ray observatory using Cherenkov telescopes, *PoS ICRC2025* (2025) 558. doi:10.22323/1.501.0558.
- [8] D. Heck, J. Knapp, J. N. Capdevielle, G. Schatz, T. Thouw, COR-SIKA: a Monte Carlo code to simulate extensive air showers., *Report FZKA 6019*, Forschungszentrum Karlsruhe (1998).
- [9] M. Bleicher, et al., Relativistic hadron hadron collisions in the ultra-relativistic quantum molecular dynamics model, *J. Phys. G* 25 (1999) 1859–1896. doi:10.1088/0954-3899/25/9/308.
- [10] S. Ostapchenko, Monte Carlo treatment of hadronic interactions in enhanced Pomeron scheme: I. QGSJET-II model, *Phys. Rev. D* 83 (2011) 014018. doi:10.1103/PhysRevD.83.014018.

- [11] K. Bernlöhr, Simulation of imaging atmospheric Cherenkov telescopes with CORSIKA and sim_telarray, *Astropart. Phys.* 30 (3) (2008) 149–158. doi:[10.1016/j.astropartphys.2008.07.009](https://doi.org/10.1016/j.astropartphys.2008.07.009).
- [12] R. Conceição, L. Gibilisco, M. Pimenta, B. Tomé, Gamma/hadron discrimination at high energies through the azimuthal fluctuations of air shower particle distributions at the ground, *JCAP* 10 (2022) 086. doi:[10.1088/1475-7516/2022/10/086](https://doi.org/10.1088/1475-7516/2022/10/086).
- [13] A. Berk, P. Conforti, R. Kennett, T. Perkins, F. Hawes, J. van den Bosch, Modtran® 6: A major upgrade of the modtran® radiative transfer code, in: 2014 6th Workshop on Hyperspectral Image and Signal Processing: Evolution in Remote Sensing (WHISPERS), 2014, pp. 1–4. doi:[10.1109/WHISPERS.2014.8077573](https://doi.org/10.1109/WHISPERS.2014.8077573).
- [14] J. Juryšek, T. Tavernier, V. Novotný, P. Hamal, M. Heller, J. Blažek, A. Muraczewki, S. R. Muthyalu, C. Alispach, Y. Renier, V. Coco, sst1mpipe: v0.7.3. 5 February 2025, Zenodo (Feb. 2025). doi:[10.5281/zenodo.14808846](https://doi.org/10.5281/zenodo.14808846).
- [15] L. Breiman, Random Forests, *Machine Learning* 45 (1) (2001) 5–32. doi:[10.1023/A:1010933404324](https://doi.org/10.1023/A:1010933404324).
- [16] R. Conceição, P. J. Costa, L. Gibilisco, M. Pimenta, B. Tomé, The gamma/hadron discriminator LCM in realistic air shower array experiments, *Eur. Phys. J. C* 83 (10) (2023) 932. doi:[10.1140/epjc/s10052-023-12106-5](https://doi.org/10.1140/epjc/s10052-023-12106-5).
- [17] A. Bakalová, R. Conceição, L. Gibilisco, V. Novotný, M. Pimenta, B. Tomé, J. Vícha, Azimuthal fluctuations and number of muons at the ground in muon-depleted proton air showers at PeV energies, *Phys. Rev. D* 111 (8) (2025) 083036. doi:[10.1103/PhysRevD.111.083036](https://doi.org/10.1103/PhysRevD.111.083036).
- [18] R. Conceição, P. J. Costa, L. Gibilisco, M. Pimenta, B. Tomé, High resolution gamma/hadron and composition discriminant variable for water-Cherenkov detector cosmic-ray observatories, *Phys. Rev. D* 110 (2) (2024) 023033. doi:[10.1103/PhysRevD.110.023033](https://doi.org/10.1103/PhysRevD.110.023033).
- [19] Z. Cao, et al., The Large High Altitude Air Shower Observatory (LHAASO) Science Book (2021 Edition), arXiv e-prints (May 2019). doi:[10.48550/arXiv.1905.02773](https://doi.org/10.48550/arXiv.1905.02773).
- [20] K. Bernlöhr, et al., Monte Carlo design studies for the Cherenkov Telescope Array, *Astropart. Phys.* 43 (2013) 171–188. doi:[10.1016/j.astropartphys.2012.10.002](https://doi.org/10.1016/j.astropartphys.2012.10.002).
- [21] C. Alispach, et al., Stereo performance of SST-1M at different altitudes, *PoS ICRC2025* (2025) 908. doi:[10.22323/1.501.0908](https://doi.org/10.22323/1.501.0908).
- [22] F. Aharonian, et al., Calibration of the air shower energy scale of the water and air Cherenkov techniques in the LHAASO experiment, *Phys. Rev. D* 104 (2021) 062007. doi:[10.1103/PhysRevD.104.062007](https://doi.org/10.1103/PhysRevD.104.062007).
- [23] D. Mandát, CTAO MST back-coated mirrors development., *PoS ICRC2025* (2025) 745. doi:[10.22323/1.501.0745](https://doi.org/10.22323/1.501.0745).
- [24] Z. Cao, et al., Data quality control system and long-term performance monitor of LHAASO-KM2A, *Astropart. Phys.* 164 (2025) 103029. doi:[10.1016/j.astropartphys.2024.103029](https://doi.org/10.1016/j.astropartphys.2024.103029).